Overvoltage Mitigation during Critical Three-Phase Faults on Half-Wavelength Transmission Lines

J.A. Santiago Ortega, M.C. Tavares

***Abstract*-- The half-wavelength transmission lines are recognized as an alternative to bulk power transmission over very long distance for its good steady state properties. However, the critical faults that can produce severe overvoltage profile on this line are an issue that must be studied. This paper presents a methodology to mitigate the severe overvoltage during critical three-phase faults using spark gaps. First, a detailed theoretical explanation of this critical overvoltage phenomenon is introduced and then an overvoltage mitigation method based on three spark gaps adequately located and coordinated is presented and tested with PSCAD/EMTDC simulations. The results are promising, showing a considerable reduction in magnitude of maximum overvoltages.**

***Keywords*: Balanced fault, half-wavelength, overvoltage, resonance, transient, transmission line.[1]**

I. Introduction

THE transmission line with half-wavelength (HWL) properties is an AC non-conventional alternative to bulk power transmission over very long distances. HWL transmission line has naturally 2500 km for 60 Hz systems and 3000 km for 50 Hz systems and it can get flexible distance using tuning procedure [1]. For this reason, it has been the focus of recent researches in continental countries like Brazil, China and Russia. These countries need strong links of 2000 km to 3000 km to deliver power from new energy sources to main load centers [2], [3]. HWL lines have excellent steady state transmission properties like a good voltage regulation with a natural reactive power balance [4], [5]. When designed with an optimized tower geometry, HWL line becomes cheaper than an equivalent HVDC line due to non-use of power electronic converters [6], [3].

However, some operative issues of HWL lines need further studies. Tradition protection elements and its algorithms do not work straightforward on HWL lines due to different behavior of voltage and currents during faults applied along the line. In this field, some alternatives for fault location using an adapted impedance algorithm [7] and traveling wave theory [8], and a new faulty phase selector has been studied with good results. In addition, non-conventional single-phase reclosing schemes have been proposed with promising results [9]. It is also known that faults at some locations produce severe overvoltage profiles that are not found on AC lines with conventional distances [10]. It is also reported that these critical faults without any mitigation method can produce instability conditions for power systems [11].

Therefore, a fundamental operational issue of HWL lines that must be studied is the phenomenon related to different behavior of voltage and current during the critical faults occurrence. This phenomenon is associated to a positive sequence resonant condition. Although three-phase fault rarely occurs in extra- and ultra-high voltage transmission lines, being the line-to-ground (LG) the most frequent one [9], the resonance condition will also occur for line-to-line faults with similar severity level, and in a smaller degree for line-to-line to ground faults, as the last one involves zero sequence circuit.

For this reason, this paper focuses on the study of critical three-phase faults and presents an improved study of overvoltage mitigation method based on spark gaps. Spark gap (SG) installed conveniently can diminish critical overvoltage [12]. To analyze it, first a theoretical analysis of HWL line under fault condition presents more insight about the series resonance phenomena and the different overvoltage profiles. Critical point of faults, maximum overvoltage levels and typical voltages profiles are clearly identified. Then, a more detailed fault study is performed and maximum transient voltage values are obtained with PSCAD/EMTDC software. The overvoltage level due to critical faults is high enough to jeopardize the insulation levels along the line and on substation terminals. Finally, an improved method to mitigate very high overvoltage using three spark gaps is proposed and tested. An explanation for the criteria to locate and specify the SGs is introduced. The obtained results are promising as overvoltage levels are reduced significantly.

II. Test System

This paper presents a study system based on a source to grid system composed a 800 kV 2600-km line (a little longer than an exact half-wavelength line - HWL+) with high surge impedance loading (SIL), which improves the transmission capacity with competitive right of way. The tower design is optimized to achieve a high SIL by modifying the bundle geometry compared with traditional lines [13]. This non-conventional line has 8 conductors per phase and the bundle geometry is shown in Fig. 1. The SIL is 4745 MW. Table 1 shows the positive/negative and zero sequence parameters for 60 Hz.

A theoretical analysis for network frequency resonance is performed in section 3 by using electrical circuit analysis and the well-known two-port network approach. Further transient analysis is performed in section 4 with PSCAD/EMTDC software using the phase-domain frequency-dependent line model. During the entire analysis, the line is adequately split

[1]This work was supported by a grant from the São Paulo Research Foundation, (FAPESP no. 2015/13823-0, 2017-20010-1), CNPq and CAPES, Brazil.
J.A. Santiago and M.C. Tavares are with the School of Electrical and Computer Engineering, University of Campinas (UNICAMP), Av. Albert Einstein, 400, 13083-250, Campinas, SP, Brazil.
e-mail: javiersa@dsce.unicamp.br, ctavares@unicamp.br).

Paper submitted to the International Conference on Power Systems Transients (IPST2019) in Perpignan, France June 17-20, 2019.

into sub-sections of shorter length for following purposes: to obtain the voltage profile along the line and to apply sliding faults at different locations. Because those cases need short line length representation (between 50 km and 100 km), no problem associated to modelling a line with such a long length was observed.

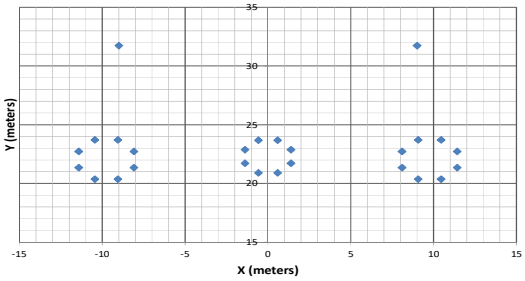

Fig.1. Tower geometry. Conductors with average height.

TABLE I
TRANSMISSION LINE PARAMETERS - CALCULATED FOR 60 HZ

Electrical parameters		
Zero sequence		
R0 (Ω /km)	X0 (Ω/km)	B0 (μS/km)
0.3871	1.3502	4.066
Positive/negative sequence		
R1 (Ω /km)	X1 (Ω /km)	B1 (μS/km)
0.0068	0.1737	9.5367

TABLE II
POWER SYSTEM PARAMETERS

Source equivalent impedances				
Source	Zero Sequence (Ω)			
Generation – 15 kV	0.000754 + j 0.025904			
Strong System – 500 kV	7.2169 + j 36.084			
Source	Positive/Neg. Sequence (Ω)			
Generation – 15 kV	0.000754 + j 0.025904			
Strong System – 500 kV	1.1864 + j 7.1187			
Equivalent transformer				
Transformer	Xr (%)	kV	MVA	Connection
T1	11.84	800/15	5197.5	Y-D
T2	10.00	800/500	4500.0	Y-Y

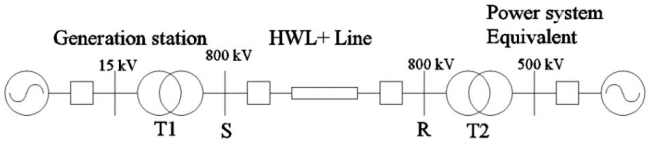

Fig.2. Power system under study.

The analyzed transmission system connects a generation station to grid (strong power system). The generation station has 11 synchronous machines with step-up transformers that produced a three-phase short circuit-current (Scc) of 9.6 kA. The individual machine parameters are based on a real generation station (Serra da Mesa, Brazil). The strong equivalent system at grid side is based on a typical 500 kV three-phase Scc of the Brazilian power system: 40 kA. Table 2 shows the network parameters. Fig. 2 shows the single-line test system diagram.

III. FAULT ANALYSIS OF HALF-WAVELENGTH POWER TRANSMISSION LINES

In this section, a theoretical analysis is introduced to learn why faults applied at some regions of HWL+ transmission line provoke resonance condition. Critical points of faults are identified and maximum voltage levels and profiles are shown. In the sequence, an overvoltage mitigation methodology is proposed.

A. Half-wavelength transmission line properties

The wavelength λ of a transmission line is calculated by (1), where β is the imaginary part of propagation constant γ, shown in (2). Z and Y are the series impedance and the shunt admittance per unit length, respectively, and ω is the angular power frequency. For a balanced three-phase transmission line, using two-port network theory with ABCD parameters, the positive sequence voltage and current along the line are described by (3), where Z_C is the positive sequence characteristic impedance and x is the distance from sending end.

$$\lambda = \frac{2\pi}{\beta} \tag{1}$$

$$\gamma = \sqrt{ZY} = \sqrt{(R + j\omega L)(G + j\omega B)} = \alpha + j\beta \tag{2}$$

$$\begin{bmatrix} V_{(x)} \\ I_{(x)} \end{bmatrix} = \begin{bmatrix} \cosh(\gamma.x) & -Z_c \operatorname{senh}(\gamma.x) \\ -\frac{1}{Z_C}\operatorname{senh}(\gamma.x) & \cosh(\gamma.x) \end{bmatrix} \cdot \begin{bmatrix} V_s \\ I_s \end{bmatrix} \tag{3}$$

Equation 3 is used to calculate the voltage and current profile along the HWL+ line for different loading levels, as shown in Fig. 3. The voltage at both line ends is approximately 1.0 pu, and the voltage is proportional to loading level in the middle of the line. In the case of current, it is proportional to loading in both line terminals and it is near to 1.0 pu in the center of line, whichever the loading level. This result is already presented in existing literature.

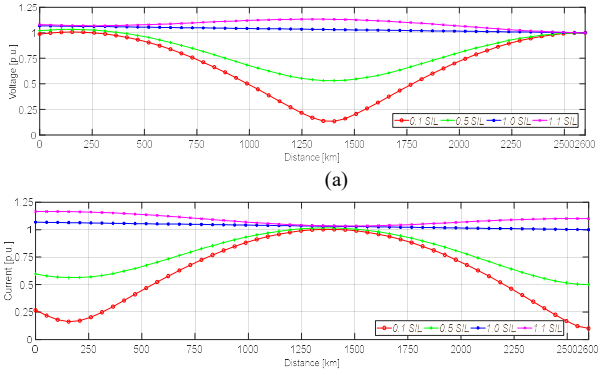

Fig. 3. Main steady-state characteristics of HWL+ transmission line for different loading levels.
(a) Voltage profile of HWL+ transmission line.
(b) Current profile of HWL+ transmission line.

B. Faults and resonance conditions on HWL+ line

Considering the wave propagation theory, the transmission line is modeled as a PI circuit with a series impedance and two shunt admittances at both ends defined by (4) and (5). This model is valid for short and long lines.

$$Z_{serie} = Zc.\sinh(\gamma.L) \tag{4}$$

$$\frac{Y_{shunt}}{2} = \frac{tanh(\gamma.{}^{L}/_{2})}{Zc} \tag{5}$$

First, we analyze the system under no-loading condition in order to observe more clearly the resonance under fault. Fig.

4.a shows a no-load HWL+ line with only one source connected (power plant) at the sending end under fault conditions. The sliding fault is modeled as a 10-Ω resistance. The three-phase fault is analyzed with the positive sequence equivalent circuit.

Fig. 4.b shows the positive sequence impedance seen by source for different fault locations. The total reactance has two zero crossings due to series resonance conditions: the first is at 1200 km, and the second is at 2166 km. The first resonance has a high resistance and there is no overcurrent. The second series resonance has almost zero resistance and thus produces higher current on the source. That is a critical resonance condition. Similar result is produced for the source at receiving terminal (considering superposition theory).

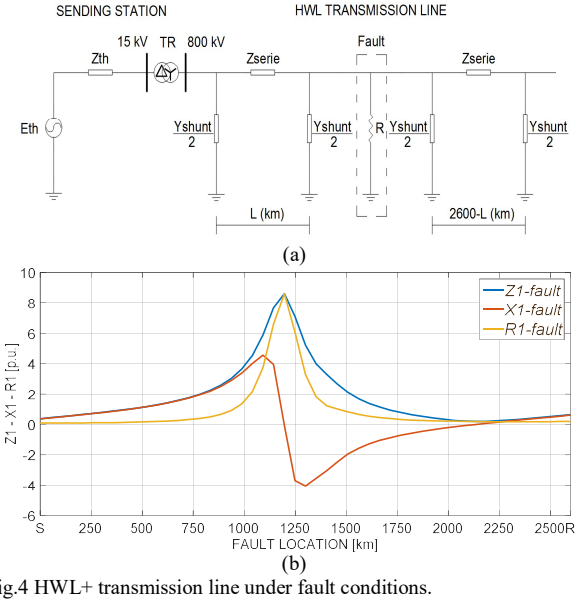

Fig.4 HWL+ transmission line under fault conditions.
(a) Equivalent circuit of the HWL line under fault conditions
(b) Equivalent positive sequence Z1, X1 and R1 seen by the source.

C. Maximum voltage values and voltage profile

Fig. 5.a shows system equivalent circuit for no-load condition after fault occurrence at 'x' km and voltage measurement at 'y' km, both from sending end. All system parameters (line and equivalent source) shown are referred to line voltage. We simplify the circuit to Fig. 5.b. In Fig 4.b the critical point of fault (x_{cpf}) that produces series resonance and the highest overcurrent is 2160 km. The location of maximum overvoltage is marked as y_{cpf}. Fig. 5.b shows the Thevenin equivalent seen by point y_{cpf}. Therefore, maximum voltage along the line for critical fault is $V_{cf\text{-}max}=V'_S.Z_B/(Z_A+Z_B)$ where V'_S is the Thevenin equivalent voltage.

For $x_{cpf} = 2160$ km the maximum voltage is at $y_{cpf} = 1000$ km. For the tested system the equivalent circuit parameters are: $V'_S = 10.4\angle -159.2°$ V_S; $Z_A = 519.9+j\ 1367.5$ Ω; $Z_B = 976.5 + j\ 534.3$ Ω.

Therefore, for sending voltage $V_S = 13.8*(800/15) = 736$ kV, the maximum voltage expected for a critical three-phase fault is $V_{cf\text{-}max} = 6.41$ pu. Here it is very important to analyze the result. This extremely high value should not be expected to occur in real life. Corona effect would appear when overvoltage starts to increase, reducing this value. Besides, TL insulation distances are not designed for such voltages higher than 3.0 pu along the TL. This maximum overvoltage value is a theoretical one and indicates a severe resonance condition.

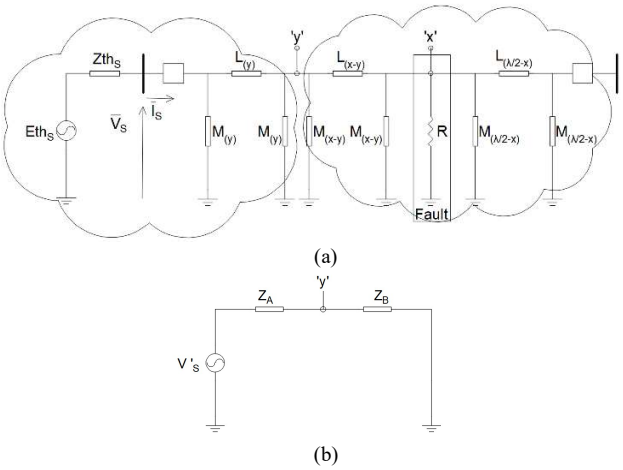

Fig. 5. Equivalent system circuit for fault condition analysis.
(a) Reduction of positive sequence circuit.
(b) Thevenin equivalent circuit

The transient circuit response shown in Fig. 6. is calculated using Simulink tool to obtain the voltage at the point with maximum overvoltage and the above voltage at sending end.

Fig. 6 shows the voltage waveforms. Sustained maximum voltage is 6.35 pu at y = 1000 km and 2.1 pu at sending end. These voltage waveforms have a high rising rate. The time constant is $\tau = 0.042$ s. Therefore, sustained response is reached in $5\tau \approx 0.210$ s.

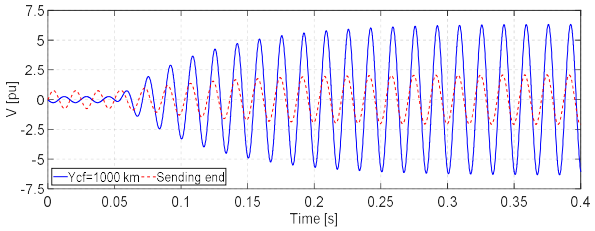

Fig. 6. Voltage waveform at maximum voltage location and sending end for most critical three-phase fault ($x_{cpf} = 2160$ km).

In order to calculate the voltage profile for critical fault, two-port network elements were used, as in Fig. 7. Sliding fault is applied along HWL at 'x' km from sending end. Eq. (6) shows the equivalent ABCD system matrices.

Equations (6), (7) and (8) with all system data were implemented in MATLAB to calculate HWL voltage profile under three-phase fault for a no-load condition. The voltage varies drastically with fault location.

$$[Q_{eq}] = [Q_{ZeqS}][Q_{TrS}][Q_{L(x)}][Q_{Fault}]\left[Q_{L\left(\frac{\lambda}{2}-x\right)}\right][Q_{TrR}][Q_{ZeqR}] \quad (6)$$

$$\begin{bmatrix} V_s \\ I_s \end{bmatrix} = [Q_{eq}]\begin{bmatrix} V_r \\ I_r \end{bmatrix} \quad (7)$$

$$\begin{bmatrix} V_s \\ I_s \end{bmatrix} = [Q_{ZeqS}][Q_{TrS}][Q_{L(Y)}]\begin{bmatrix} V_{L(y)} \\ I_{L(y)} \end{bmatrix} \quad (8)$$

where
Q_{Zeqs}: two-port network of generators.
Q_{TrS}: two-port network of transformer at sending end.

$Q_{L(X)}$: two-port network of the line with 'x' km.
Q_{Fault}: two-port network of the fault.
$Q_{L(\lambda/2-x)}$: two-port network of the line with 'λ/2-x' km.
Q_{TrR}: two-port network of transformer at receiving end.
Q_{Zeqr}: two-port network of the equivalent at receiving end.
Vs, Is: internal voltage and current of the sending generator.
Vr, Ir: internal voltage and current of the receiving equivalent source.
$V_{L(Y)}$, $I_{L(Y)}$: V and I at the point of measurement located at 'y' km from sending end.

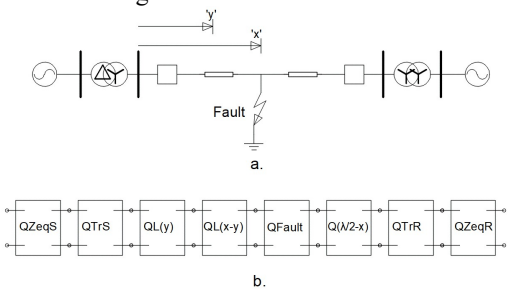

Fig. 7. Power system representation.
(a) Test system.
(b) Two-port network equivalent system.

Fig. 8.a shows the maximum voltage over the entire line for faults applied at different locations. Faults applied at 2160 km (83% of the length from source) cause the highest overvoltage. Fig. 8.b shows voltage profile for faults at 2160 km, 1800 km and 1300 km. The overvoltage level decreases as the point of fault moves away from the critical point. For worst fault, the maximum theoretical value is 6.41 pu measured at 1000 km. Fault at 1800 km presents a maximum voltage of 1.95 pu. Fault in the middle of line does not provoke overvoltage.

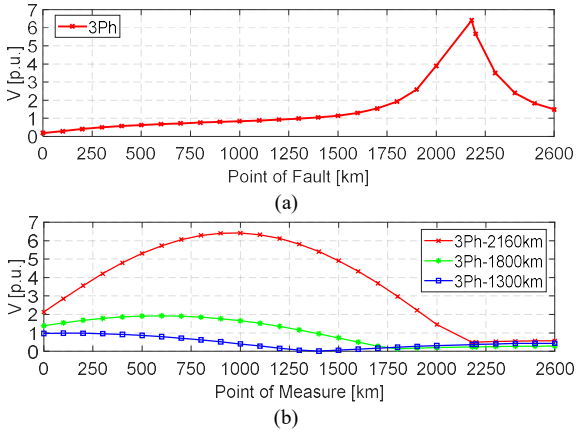

Fig. 8. Three-phase fault at HWL line in no-load condition.
(a) Maximum voltage along line for different fault locations.
(b) Voltage profile for faults at: 2160 km, 1900 km and 1300 km.

For actual operation, superposition analysis is applied summing up contribution of both terminals' sources. It is observed that faults around 83% from sending terminal promotes a resonance condition excited by source at sending end. Symmetrically, a fault around 83% from receiving end (the exact location will depend on remote end strength) provokes a resonance condition excited by remote end equivalent system. In that case the maximum overvoltage value will be observed around 1000 km from receiving end.

The fault resistance (Rf) has impact on critical faults, decreasing overvoltage value as Rf increases. For faults out of critical region Rf will have less impact because the system reactance is more relevant.

D. Detuning resonance to mitigate overvoltages

As we have seen in Fig. 5, three-phase fault on critical locations produces resonance condition resulting in severe overvoltage profile along the line.

At the beginning of the fault the voltage rate of rise is approximately 2.0 pu/cycle, as shown in Fig. 6. It means that in the second cycle after the fault, the voltage at critical point could reach values higher than typical basic switching impulse insulation levels (BSL), especially in the middle of line. A regular protection system (including the circuit-breaker opening time) takes at least 4 cycles to open the circuit. Therefore, critical three-phase fault requires a mitigation method to control the voltage until protection system trips the line.

A quick review of factors that affect resonance condition indicates that main influencing parameters are fault point, line impedance, and terminal equivalent impedance. As there is no control for the point of fault and impedances, the more appropriate action is detuning the resonance by changing the system configuration, as indicated in Std. IEEE 1313.2. For this, a fast action is needed. Elements with time response lower than one cycle are the spark gaps (SG) and impedances controlled by thyristors. Because critical faults involve sustained overvoltage with high-energy content, the use of surge arresters is disregarded [10]. It is important to observe that SG is installed at tower structure, one for each phase.

The present document introduces a mitigation method based on SG that acts as a voltage controlled grounding switch at an adequate line position, detuning the system resonance. The criteria to locate and set the sparks gaps are the following:

- The SGs must act only for critical faults. Voltage from events like energization and load rejection must not excite SG and should be coordinated with SG voltage breakdown.
- Line-to-ground (LG) fault is the most frequent one and in most cases is non-permanent. SG should not operate for this fault.
- A natural location for the spark gaps is the center of line (1300 km) because if line is grounded at this point there is no series resonance excited by neither sending nor receiving equivalent systems. No overvoltage is observed, as shown in Fig. 8.
- However, more SGs can be used to reduce conveniently the overvoltage profile. These elements can be located at points with higher voltage level, considering that the first SG to operate is the one located at the center of the line.

IV. Performance of the Mitigation Method

A. Model and simulation of system on PSCAD

This part of the study was performed with a more detailed model using PSCAD/EMTDC software. The system characteristics are:

a. Phase-domain model was used to properly represent transmission line series parameter frequency dependence.

b. Real transposition was implemented with 9 transposition cycles of 290 km each one (48-96-96-48 km).
c. Time step of 10 μs.
d. Generators at sending end with 1.0 SIL loading condition.
e. Grid side with a strong power system.
f. Transformers modeled at both substations, with saturation data: knee voltage at 1.40 pu and an air core reactance of 0.169 pu.
g. Protection trips the line 4 cycles after fault occurrence.
h. Surge arresters connected at terminals' substations.

B. Spark gaps model, location and voltage breakdown

Spark gap model is based on long electric arc model in free space [14] that can be represented by a primary arc model due to the long electrode distance. We consider the arc voltage is modeled as a source function of arc current and the arc length is constant due to the high current level [15].

The first SG is located at the central part of line (1300 km). When the line is grounded at this point, it is divided in two subsystems with a source exciting a quarter-wavelength line (λ/4). In steady state condition there is no overvoltage profile. However, electromagnetic transient simulation is necessary to evaluate the performance of SGs due to successive events: fault at critical point, next: SG operates, and eventually line tripping.

The SG voltage breakdown must coordinate with maximum voltage of LG faults, line energization and load rejection, as presented in Fig. 9. For LG faults, location and the phase involved in the line was varied, and the result shows the worst condition. In the case of energization, the results come from a statistical simulation with 100 shots and 2 ms standard deviation. In the load tripping simulation, maximum load (1.0 SIL) rejection was simulated. It can be seen that similar overvoltage profile is obtained for line energization and load tripping. At km 1300, the maximum voltage due to LG fault is 1.98 pu and for the line energization is 1.18 pu. Therefore, SG voltage breakdown at 1300 km is set to $V_{BD} = 1.98 * 1.1 = 2.17$ pu.

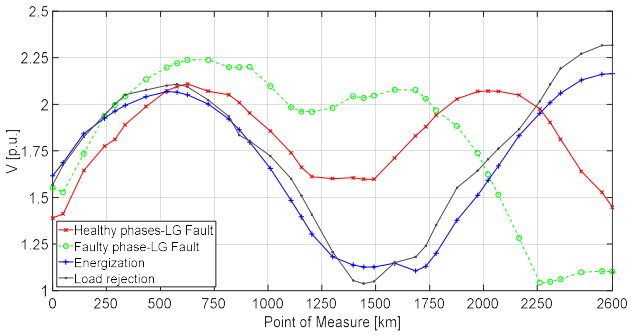

Fig. 9. Maximum voltage measured along the line due to LG faults applied along the line, line energization and load trip.

C. Performance of overvoltage mitigation system

Formerly, different faults along the line without any SG were simulated. For these cases, the maximum voltage due to faults over the entire line is 6.3 pu for fault applied at 2166 km, as shown in Fig. 10 (red line). This fault is excited by sending source. Fault at point 337 km produces a maximum voltage of 3.89 pu due to resonance excited by receiving end equivalent.

These values are lower than that calculated in last section because here regular protection time was adopted, 4 cycles, and also the terminals' transformers were modeled with saturation.

In sequence, the SG is connected at 1300 km. The maximum voltage over the entire line due to sliding faults are shown in Fig. 10.a (green line). The maximum voltage decreases in the area around critical resonant area, and the maximum values are 4.05 pu for fault at 2166 km and 3.46 pu for fault at 337 km.

An improved performance can be obtained placing two additional SGs at the points were the maximum voltages are measured for critical faults. Fig. 10.b shows the maximum voltage measured along the line for worst three-phase fault and one spark gap. The maximum values are in two regions between 50 km to 600 km and 2000 km to 2500 km. Two additional SGs are installed at 433 km and 2262 km (Fig.11). The voltage breakdown of each one was chosen as 10% higher than the former SG - at 1300 km (2.38 pu). At the same time it must be at least 10% higher than maximum restriction voltages shown in Fig. 9.

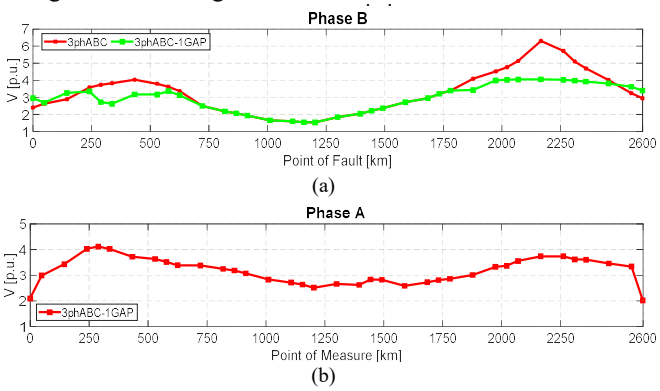

Fig. 10. Maximum voltage (MV) for different faults along the line.
(a) MV for different point of fault.
(b) MV measured along the line for worst fault.

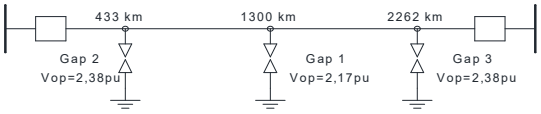

Fig. 11. HWL line with three SGs.

The system was simulated with three SGs. Fig. 12 shows the maximum voltage over the entire line due to three-phase fault applied along the line. A reduction on maximum voltages was properly achieved in the areas around critical resonant points. Finally, the maximum overvoltages were reduced to 3.5 pu for fault at 2166 km and 2.88 pu for fault at 337 km.

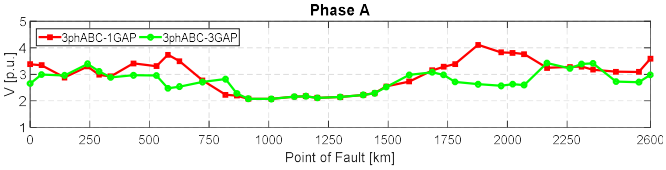

Fig. 12. MV for different faults along the line using three SGs.

Fig. 13.a and Fig. 13.b show the voltage waveforms for faults at resonant points 2166 km and 337 km, respectively. The phase with highest overvoltage is presented, specifically

phases B and A. Voltages at SGs were also included. Fig. 13.c shows the voltage waveform at sending substation when fault is applied at 2166 km. It can be observed that the voltage is now limited to 2.0 pu. In this case, phase A surge arrester energy will be 9.7 MJ.

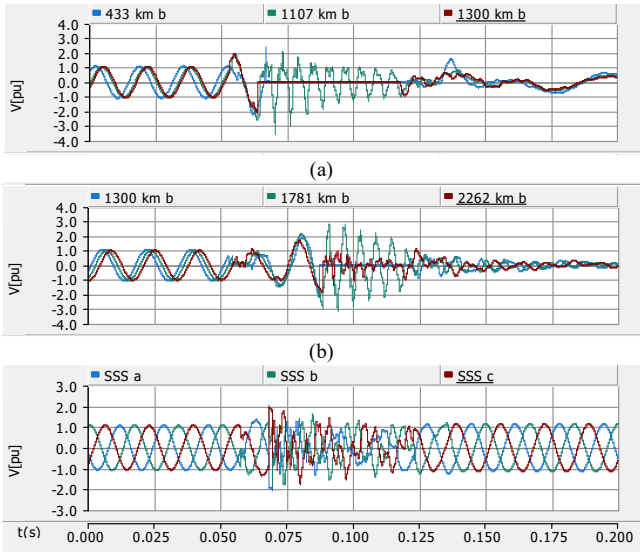

Fig. 13. Voltage waveform for worst conditions.
(a) Measured at gaps and maximum voltage locations (Fault at 2166 km).
(b) Measured at gaps and maximum voltage locations (Fault at 433 km).
(c) Measured on CB at sending substation side (Fault at 2166 km).

V. Conclusions

This paper introduces a detailed analysis of critical balanced faults associated to fundamental frequency resonance on half-wavelength transmission lines. Although balanced faults are not the most frequent for transmission lines, they will provoke extremely high overvoltages in HWL and have been identified as a major concern for this bulk AC transmission alternative.

This series resonance fault is not observed on AC lines with conventional length. Actually, it derives from the balance of inductive and capacitive response in such a very long line. When this phenomenon occurs it will produce extreme voltage and current changes.

The theoretical overvoltage levels are extreme and the voltage rate of rise is high enough to prevent the application of typical protection operation time. A mitigation procedure must be postulated.

A spark gap (SG) system composed of three elements to detune series resonance is proposed, introducing a criteria to properly locate and set the SGs. Their voltage breakdown must be coordinated with other events such as line-to-ground fault, line energization and load tripping. As a result, when three SGs are installed the resonance is properly detuned. The locations are 1300 km, 433 km and 2260 km. Regular protection operation time can then be considered. The overvoltages were controlled and are in the same level as the ones observed in AC system with regular line lengths. The SGs mitigation procedure can be applied to 60- or 50-Hz system, that is to say, for 2500 km or 3000 km long line, as well as to tuned HWL. Further studies should be implemented to analyze dynamic stability of system.

Positive sequence line parameters depend mostly on tower geometry and conductor's characteristics, what does not change drastically for UHVAC transmission lines of the same voltage level. Therefore only small changes on critical three-phase fault locations are expected for other HWL lines, although short-circuit terminal network level can shift slightly the critical location.

VI. References

[1] J. S. Ortega and M. C. Tavares, "New perspectives about AC Link based on Half-Wavelength Properties for Bulk Power Transmission with Flexible Distance," IET Gener. Transm. Distrib., vol. 12, no. 12, pp. 3005–3012, 2018.

[2] M. Tavares et al., "Power Transmission over long Distances with Half-Wavelength Technology", First Ed., São Paulo, Brazil, 2017.

[3] G. Samorodov et al., "Technical and economic comparison between direct current and half-wavelength transmission systems for very long distances," IET Gener. Transm. Distrib., vol. 11, no. 11, pp. 2871–2878, 2017.

[4] F. S. Prabhakara, K. Parthasarathy, and H. N. Rao, "Analysis of Natural Half-Wave-Length Power Transmission Lines," IEEE Trans. Power Appar. Syst., vol. PAS-88, no. 12, pp. 1787–1794, 1969.

[5] F. Iliceto and E. Cinieri, "Analysis of half-wave length transmission lines with simulation of corona losses," IEEE Trans. Power Deliv., vol. 3, no. 4, pp. 2081–2091, 1988.

[6] C. Portela, J. Silva, and M. Alvim, "Non-Conventional AC Solutions Adequate For Very Long Distance Transmission – An Alternative For The Amazon Transmission System," in IEC / CIGRE UHV Symposium, Beijing, China, 2007.

[7] F. V. Lopes, B. F. Küsel, K. M. Silva, D. Fernandes, and W. L. A. Neves, "Fault location on transmission lines little longer than half-wavelength," Electr. Power Syst. Res., vol. 114, pp. 101–109, 2014.

[8] F. V Lopes, B. F. Küsel, and K. M. Silva, "Traveling Wave-Based Fault Location on Half- Wavelength Transmission Lines," IEEE Lat. Am. Trans., vol. 14, no. 1, pp. 248–253, 2016.

[9] O. Dias and M. C. Tavares, "Single-Phase Auto Reclosing Mitigation Procedure for Half Wavelength," IET Gener. Transm. Distrib., vol. 11, no. 17, pp. 4324 – 4331, 2017.

[10] F. M. Gatta and F. Iliceto, "Analysis of some operation problems of half-wave length power transmission lines," in IEEE Conference Publications - 3D Africon Conference. Africon '92 Proceedings (Cat. No.92CH3215), 1992, pp. 59–64.

[11] Z. Xu, J. Yang, and N. Sheng, "Infeasibility Analysis of Half-Wavelength Transmission Systems," Energies, vol. 11, no. 7, p. 1790, 2018.

[12] J. Santiago and M. C. Tavares, "Analysis of half-wavelength transmission line under critical balanced faults: Voltage response and overvoltage mitigation procedure," Electr. Power Syst. Res., vol. 166, pp. 99-111, Oct. 2018.

[13] J. S. Acosta and M. C. Tavares, "Methodology for optimizing the capacity and costs of overhead transmission lines by modifying their bundle geometry," Electr. Power Syst. Res., vol. 163, pp. 668-677, Oct. 2017.

[14] V. V. Terzija, R. Ćirić, and H. Nouri, "Improved fault analysis method based on a new arc resistance formula," IEEE Trans. Power Deliv., vol. 26, no. 1, pp. 120–126, 2011.

[15] J. Talaisys, M. C. Tavares, C. Portela, A. Câmara, "Estimation of Length Variation of Artificially Generated Electrical Arc in Out-Door Experiment", International Conference on Power Systems Transients (IPST'11), Delft, Holland, 14-17 June, 2011.